Lithium isotope evidence for enhanced hydrological cycling during Oceanic Anoxic Event 2

Philip A.E. Pogge von Strandmann[1*], Hugh C. Jenkyns[1] and Richard G. Woodfine[1†]

[1]Department of Earth Sciences, University of Oxford, South Parks Road, Oxford, OX1 3AN, UK

*Contact email: philipvs@earth.ox.ac.uk

[†]Current address: BP, Chertsey Road, Sudbury-on-Thames, UK

The Cenomanian–Turonian Oceanic Anoxic Event (~93.5Ma) represents a period of rapid global warming, high atmospheric CO_2 and marine anoxia/euxinia for ~440kyr, leading to habitat loss and mass extinction. Although this anoxia can be explained by enhanced biological productivity, it is unclear how this phenomenon was triggered, and what allowed rapid climatic recovery from this warm period. Here we reconstruct changes in ocean chemistry caused by silicate rock weathering, a significant climate moderating and nutrient supply process, via lithium isotope ratios (δ^7Li) in marine carbonates. The largest δ^7Li excursion and lightest values yet measured in marine carbonate suggest enhanced rates of hydrological cycling, weathering and CO_2 removal during the OAE. Models of Li and other isotopic tracers (Ca, Sr, Os) suggest that the eruption of a large igneous province led to high atmospheric pCO_2 and rapid global warming (which initiated the OAE) as well as a transitory ~200kyr pulse of accelerated mafic silicate weathering rates. This latter process, together

with organic-matter burial, led to CO_2 drawdown, allowing rapid recovery and stabilisation from an enhanced greenhouse state.

Oceanic Anoxic Event 2 (OAE2) at the Cenomanian–Turonian (C–T) boundary at ~93.5Ma is thought to represent one of the warmest periods of the Phanerozoic[1], with high atmospheric CO_2 levels[2] and sea-surface temperatures[3], low pole–Equator temperature gradients, and a resulting mass extinction caused by deterioration of ecological space[4]. OAE2 is also characterised by widespread deposition of black shale, interpreted to result from global oceanic anoxia and/or euxinia and very high burial rates of marine organic carbon, causing a positive $\delta^{13}C$ excursion[5] in the ocean–atmosphere system lasting some 430-445kyr[6]. Anoxia/euxinia is also suggested by concentration changes in certain biomarkers, redox-sensitive metals, as well as perturbations in redox-sensitive isotope systems[1]. Given that the C–T OAE corresponds with a relative palaeotemperature maximum[3], it is likely that it was accompanied by acceleration of the hydrological cycle and increased global weathering rates. Indeed, a possible chain of events triggering the phenomenon may have been increased atmospheric CO_2 from the emplacement of the Caribbean, Madagascar and/or parts of the Ontong-Java Plateaux[5], which led to enhanced weathering and consequent high nutrient input to the oceans, stimulating biological productivity and accelerated carbon flux to the sea floor, thus fostering the OAE[1]. Termination of the OAE may have been forced by sequestration of CO_2 by both silicate weathering and photosynthetic fixation into sedimentary organic matter, causing final slowing of the hydrological cycle. Evidence of enhanced continental weathering has been proposed from brief radiogenic $^{87}Sr/^{86}Sr$ excursions[7] and

trends towards lighter Ca isotopes[8], before both Sr and $^{187}Os/^{188}Os$ dropped to relatively unradiogenic values throughout the OAE[9]. However, all of these isotopic systems are subject to interpretational ambiguity, due to potential variations in the isotope ratio of weathered lithologies in the continents, and the relative proportions of both carbonates and silicates, where only weathering of the latter affects atmospheric CO_2 on geological timescales[10-12]. Processes such as ocean acidification, calcification rate and temperature can also affect Ca isotopes[13].

Influence of weathering on river and oceanic Li isotope ratios

Understanding the timing and tempo of continental weathering is critical for testing the OAE model, and for evaluating the role of CO_2 drawdown in climatic stabilisation. We investigate this phenomenon in the context of the C–T OAE by using stratigraphic variations in the Li isotope ratio (δ^7Li), a relatively novel tracer for silicate weathering[14-17]. Lithium is almost totally situated in silicates and silicate secondary minerals so that, even in carbonate-rich catchments, Li is entirely dominated by weathering of silicate rocks[18,19]. The δ^7Li of primary silicate rocks defines a narrow range (average basalt ~2–5‰; average continental crust ~0‰[17,20,21]); consequently, given the high variability of δ^7Li in modern rivers (6–42‰; average ~23‰[16,17]), fluvial δ^7Li is effectively independent of silicate lithology. Lithium isotopes are also not fractionated by uptake into plants[16,22], and the variable δ^7Li of rivers is due to preferential uptake of ^6Li by secondary clay minerals[16]. The δ^7Li of rivers thus reflects mixing between two end-member solutes: one formed by primary silicate mineral dissolution (with low δ^7Li and high [Li]) and the other related to secondary

mineral formation (with high δ^7Li and low [Li])[18,23,24]. Thus, a high riverine Li flux can be used as a tracer of high silicate weathering rates (mass of rock dissolution per unit area and time), while a low δ^7Li represents high chemical weathering intensity (or degree of weathering, defined as the ratio of material supplied to the oceans by primary mineral dissolution relative to that retained by secondary mineral formation)[14]. Hence, if the weathering regime is weathering-limited (thin soils and hence incongruent weathering, with chemical reactions controlled by temperature and runoff)[25], dissolved δ^7Li is expected to be highly fractionated from the host rock, with relatively more Li taken up into clays[14,26-28], whereas if the regime is transport-limited (thick soils, with weathering rates limited by the physical supply of material, an equilibrium between soils and clays, and hence more congruent weathering [23,25]), δ^7Li will be similar to rock values[14].

In modern oceans, continental weathering represents ~50% of the Li ocean input, with the other ~50% contained in hydrothermal solutions expelled at mid-ocean ridges (high temperature weathering of basalts), whose δ^7Li is ~8‰[26,27]. The main sink for Li is from incorporation into low-temperature clays in altered basalt and marine sediments, which have a cumulative present-day isotopic fractionation factor of α ~0.985, driving modern seawater δ^7Li to a value of 31‰[17]. Importantly, marine carbonates represent a negligible sink for Li, and the isotopic fractionation factor remains approximately constant at ~3–5‰, is independent of temperature or salinity, and does not differ in inorganic and all types of skeletal calcite (see Supplementary Information for details).

Li isotope variations across the OAE

For this study, bulk calcite samples were measured for trace metals and Li isotopes in a stratigraphically expanded Cenomanian–Turonian section through the nannofossil-rich English Chalk exposed at Eastbourne, UK[29]; at South Ferriby, UK, where a more condensed Chalk section[30] is interrupted by a depositional hiatus; and a Cenomanian–Santonian rudist-bearing shallow-water limestone at Raia del Pedale, southern Italy[4] (Fig. 1). Both English sections were deposited in a shallow epicontinental pelagic shelf sea, whereas the Italian section represents a carbonate platform installed on the Tethyan continental margin. All three sections have been extensively analysed for C, O, Ca and Sr isotopes[4,8,31]. The Cenomanian–Turonian boundary in these sections can be readily correlated with other localities, including the Global Boundary Stratotype Section and Point (GSSP) for the base of the Turonian stage exposed in Colorado, USA, through macro- and microfossil biostratigraphy and carbon isotope stratigraphy[32]. The three European sections show initial (pre-carbon isotope excursion) δ^7Li values of ~20‰, (Fig. 2). The δ^7Li minimum (6–10‰) in all sections occurs within the carbon isotope excursion and, in the stratigraphically expanded Eastbourne section, δ^7Li values recover to pre-excursion values more rapidly than do the C isotopes themselves. Post-excursion δ^7Li values tend to be similar to pre-excursion values, and also similar to foraminiferal carbonate values of ~27‰ recorded from the Maastrichtian stage ~23Myr later[27]. δ^7Li from apparently correlative parts of the sections do differ slightly (Fig. 3), possibly suggesting some local variation in watermass geochemistry due to differences in ocean circulation[33] or more probably reflecting the partially incomplete nature of some the records, as is manifestly the case at South Ferriby (Fig. 2). All sections also exhibit contemporaneous Li/Ca increases.

Isotopic constraints on Cretaceous seawater chemistry

Processes that could cause relatively light δ^7Li in carbonate are 1) leaching of clays during sample processing; 2) diagenesis, including cation exchange with isotopically light silicate clays; 3) a primary seawater signal, driven either by an increase in the hydrothermal flux, variations in the riverine flux or fluvial δ^7Li, or combinations of all three. Cation exchange or leaching of clays prior to analysis was monitored by analysing cation/Ca ratios of the calcite samples. Various leaching experiments were performed, and comparisons were also made between δ^7Li and lithostratigraphy (see supplementary information). No obvious relationship between δ^7Li and stratigraphic variations in clay content is discernible. We can similarly discount diagenesis, because both similar trends and absolute values are repeated in sections from different palaeogeographic settings, and potentially reactive pore waters from hemipelagic sediments have been shown to be isotopically heavy[34-36]. Furthermore, C, O and Sr isotopes show similar values in these different profiles and compare well with other sections across the Cenomanian–Turonian boundary[37]. It is suggested, therefore, that the isotopic shifts in the carbonate sections must represent primary seawater signatures.

In order to constrain the cause of the decrease in seawater δ^7Li, we combine Li isotopes with Sr, Os and Ca isotopes, measured either on the same samples, or in sections that can be correlated at high resolution using carbon isotope stratigraphy[8,9,37]. Thus Sr isotopes show a well-constrained ~4Myr trend to less radiogenic values, with a brief radiogenic spike reported in one section at the inception of the carbon isotope excursion[7]. Unradiogenic Os-isotope ratios only persist for the duration of the OAE, with no radiogenic spike yet reported[9].

Finally, Ca isotopes ($\delta^{44/40}Ca$) show a 0.3–0.5‰ decrease, also for the duration of the carbon isotope excursion[8] (Fig. 2). The combination of these tracers utilised in a series of dynamic models can thus provide constraints on the processes causing and operating within the OAE. We use the unradiogenic long-term $^{87}Sr/^{86}Sr$ trend to constrain the hydrothermal input, because Sr isotopes are the most sensitive of these systems to this flux, and δ^7Li to understand the silicate weathering input (see supplemental information for model details). Thus the $^{87}Sr/^{86}Sr$ record suggests that the hydrothermal input increased by ~20% for 4Myr. However, this process would only have driven seawater δ^7Li lighter by some 0.5‰, which presupposes that a change in silicate weathering must also have occurred. A constant Li river flux accompanied by decreased δ^7Li (i.e. constant weathering rates but increased weathering intensity) for 200kyr (in order to allow seawater δ^7Li recovery within 430kyr) would also only result in seawater values ~1‰ lighter. Equally, if the river δ^7Li were kept constant, then the fluvial flux would have had to increase >50× to cause the observed isotopic shift (see supplementary information). Although seawater Li concentrations cannot be constrained from Li/Ca because of additional controls by temperature and salinity[13,38], the increase during the OAE shown in all sections suggests that it is unlikely that seawater [Li] increased by more than a factor of 5.

Thus, modelling the observed Li and Sr isotope excursions requires a 4Myr 20% increase in the hydrothermal flux, and a ~200kyr pulse of enhanced riverine Li flux coupled with very light (river δ^7Li ~2–4‰) fluvial isotope ratios (Fig. 4). This combined increase in river flux and decrease in δ^7Li most probably records increased silicate weathering rates and a shift to a transport-limited,

intense weathering regime. In the expanded Eastbourne section, δ^7Li shows at least two distinct pulses of light isotope ratios, suggesting variation in the weathering intensity. Estimates of palaeo-SST also show irregularities in temperature, likely associated with pCO_2 changes[3]. It is possible that these changes caused the observed Li isotope variations. Alternatively, this signal may be due to massive destabilisation of continental secondary minerals, also causing addition of isotopically light Li, as well as other cations, to the oceans. In either case, movement to lower δ^7Li indicates large changes in the hydrological cycle.

Additional constraints to the model can then be brought to bear, using Ca and Os isotopes. Significantly, $^{187}Os/^{188}Os$ in rivers would not be driven to very unradiogenic values by the destabilisation of secondary clays[39]. Given that the hydrothermal flux is constrained by $^{87}Sr/^{86}Sr$, the decrease in $^{187}Os/^{188}Os$ to ~0.17[9] must have been caused by weathering of unradiogenic, mantle-derived rocks such as basalts (see Supplementary Information), rather than radiogenic continental crust. Generally, the pre-OAE Cenomanian climate is thought to have been warm, with low-lying peneplained continents[40,41] and relatively thick soils. Thus, in order to increase weathering rates dramatically, fresh mineral surfaces must have been provided at the C–T boundary. In fact, all four isotope systems can be modelled by combining a 4Myr 20% increase in the hydrothermal flux, combined with a ~200kyr pulse of increased riverine flux from basaltic rocks, associated with a brief but intense transport-limited weathering regime (Fig. 4), although in this case the "transport" limitation was likely the availability of fresh mafic material, allowing rapid, congruent chemical weathering. The degree of increase in river flux of each element has been estimated from their relative proportions in modern rivers draining basaltic igneous provinces such as Iceland

and the Azores, and is also dependent on estimates of ocean residence time. Given likely reduced pre-OAE riverine fluxes, higher mid-ocean ridge spreading rates (i.e., more basalt available for low-temperature alteration) and different calcite precipitation rates, lower residence times relative to the present-day are probable for some elements, and have been proposed for Sr[7]. Such marine chemistry would also explain the observed relatively fast response times of the isotopic systems (Fig. 4), and also allows smaller changes in the riverine fluxes during the OAE.

Implications of enhanced weathering during OAE2

Thus the model suggests that explaining the Li isotope data requires the riverine flux to increase ~2–4 times during the OAE in the presence of a lower oceanic Li residence time relative to the present-day. Given the demonstrated response of lighter dissolved δ^7Li with increasing modern basaltic weathering rates[14,24,42], the eruption of subaerial basalts just prior to the onset of OAE2 is the most logical choice to explain the isotopic variations. Evidence from coupled C and Pb isotopes has been taken to suggest that there was massive subaerial volcanism during OAE2 linked to the Caribbean or Madagascar Large Igneous Provinces, releasing significant amounts of basalt as well as volcanic ash onto the continents[43], where the weathering of both will initially release light Li[14,28,44]. Equally, LIP formation would have exposed fresh basalt to weathering by seawater, and hence it is possible that both shallow marine and subaerial weathering of basalt contributed to the isotopic signals[43]. Modern rivers draining both basaltic and continental crust lithologies show trends of increasing Li concentration with silicate weathering rate[19,42]. If the weathering-rate weighted

average of the river concentrations is calculated, then basaltic catchments are ~50% lower than those on continental crust, suggesting that to create a 2–4-fold increase in a basalt-derived Li flux, total silicate weathering rates from submarine and subaerial basalts must have increased ~1–3 times. This estimate is similar to rate increases inferred from modelled increases in nutrient fluxes[45]. Freshly erupted basalts tend to be prone to high weathering rates due to availability of volcanic glass[24], and because secondary minerals have not yet precipitated to any great degree[46]. Indeed, the degradation of modern basalts has been shown to have a disproportionately high effect on both subaerial and marine chemical weathering and particle supply to the oceans[47], processes that will sequester atmospheric CO_2[14,16,47].

The stratigraphically expanded Eastbourne section suggests that mafic silicate weathering started to increase ~30kyr before the onset of OAE2, based on its estimated duration of 445kyr[6]. This interval is of similar duration to the ~23kyr proposed between the onset of relatively unradiogenic values of $^{187}Os/^{188}Os$ and the OAE itself[9]. Thus the data and models combined suggest that massive subaerial and shallow-marine volcanism increased the pCO_2 concentration of the atmosphere, triggering global warming and causing an intensification of the hydrological cycle, in turn promoting an increase in basaltic weathering rate and weathering intensity in both subaerial and marine realms, with the overall system becoming more transport-limited. The direction of δ^7Li fractionation is the same as that reported at the Cretaceous–Palaeocene boundary, when weathering is also proposed to have become more transport-limited, and the riverine flux increased[27]. However, the magnitude of the isotopic shift observed at the C–T OAE is ~2.5 times greater, and has less than half the

duration. The modelled increase in riverine Li flux necessitates the dissolution by weathering of ~0.6–2×10^6 km^3 of basalt[14,24,28], which represents ~10–40% of individual LIPs thought to be erupting at that time (Caribbean, Madagascar or Ontong Java Phase 2)[43,48]. The congruent nature of the weathering during the OAE, and the tracer for silicate weathering given by the Li system, allows calculation of the amount of CO_2 that would have been sequestered[49]. Hence, during dissolution of this amount of basalt, ~4–8×10^4 Gt CO_2 was likely consumed, which is of a similar magnitude, albeit slightly lower, than the 7–12×10^4 Gt CO_2 calculated to have been released during initial Cenomanian-Turonian volcanism[43,50]. The latter calculation was based on C isotopes, and hence may be a minimum estimate, given that the $\delta^{13}C$ value of the ocean–atmosphere system will have been affected by competing volcanism and carbon burial. However, this study suggests that in excess of a third of the emitted CO_2 was effectively balanced by silicate weathering by the end of the oceanic anoxic event, given that a significant amount of carbon was demonstrably sequestered within OAE black shales. Approximately 200–300kyr after the start of volcanism, basaltic silicate weathering reached its peak, and subsequently began to decline, leading to a more weathering-limited regime (increased δ^7Li, similar to the long-term Eocene to present δ^7Li trend[27]), reaching pre-eruption levels ~100kyr (Eastbourne) to ~300kyr (Raia del Pedale) later (Fig. 3), and allowing the oceans to begin a gradual recovery to more oxic conditions. Hence, these data also suggest that the hydrological cycle and chemical weathering can reach a peak, consume a significant amount of CO_2, and decline within ~300kyr.

Additional information:

Correspondence should be addressed to P.P.v.S., while requests for materials to H.C.J.

Acknowledgements:

Nick Belshaw and Phil Holdship are thanked for assistance with developing the isotope ratio and trace element analysis methods. Clara Blättler is thanked for discussions on Ca isotopes. PPvS is funded by NERC Research Fellowship NE/I020571/1. This manuscript was greatly improved by comments from Sambuddha Misra and three anonymous reviewers.

Author contributions

P.P.v.S. performed the Li isotope and trace element analyses, wrote the manuscript and constructed the models. H.C.J. collected the samples and edited the manuscript. R.G.W. measured Sr isotope data from Raia del Pedale.

1 Jenkyns, H. C. Geochemistry of oceanic anoxic events. *Geochem. Geophys. Geosyst.* **11**, Q03004, doi:10.1029/2009GC002788 (2010).

2 Sinninghe Damsté, J. S., Kuypers, M. M. M., Pancost, R. D. & Schouten, S. The carbon isotopic response of algae, (cyano)bacteria, archaea and higher plants to the late Cenomanian perturbation of the global carbon cycle: Insights from biomarkers in black shales from the Cape Verde Basin (DSDP Site 367). *Organic Geochemistry* **39**, 1703–1718 (2008).

3 Sinninghe Damsté, J. S., van Bentum, E. C., Reichart, G. J., Pross, J. & Schouten, S. A CO_2 decrease-driven cooling and increased latitudinal temperature gradient during the mid-Cretaceous Oceanic Anoxic Event 2. *Earth Planet. Sci. Lett.* **293**, 97–103, doi:10.1016/j.epsl.2010.02.027 (2010).

4 Parente, M. *et al.* Stepwise extinction of larger foraminifers at the Cenomanian-Turonian boundary: A shallow-water perspective on nutrient fluctuations during Oceanic Anoxic Event 2 (Bonarelli Event). *Geology* **36**, 715–718 (2008).

5 Jones, C. E. & Jenkyns, H. C. Seawater strontium isotopes, oceanic anoxic events, and seafloor hydrothermal activity in the Jurassic and Cretaceous. *Am. J. Sci.* **301**, 112–149 (2001).

6 Voigt, S. *et al.* The Cenomanian – Turonian of the Wunstorf section – (North Germany): global stratigraphic reference section and new orbital time scale for Oceanic Anoxic Event 2. *Newsletters on Stratigraphy* **43**, 65–89 (2008).

7 Frijia, G. & Parente, M. Strontium isotope stratigraphy in the upper Cenomanian shallow-water carbonates of the southern Apennines: Short-term perturbations of marine $^{87}Sr/^{86}Sr$ during the oceanic anoxic event 2. *Palaeogeography, Palaeoclimatology, Palaeoecology* **261**, 15–29 (2008).

8 Blättler, C. L., Jenkyns, H. C., Reynard, L. M. & Henderson, G. M. Significant increases in global weathering during Oceanic Anoxic Events 1a and 2 indicated by calcium isotopes. *Earth Planet. Sci. Lett.* **309**, 77–88 (2011).

9 Turgeon, S. C. & Creaser, R. A. Cretaceous oceanic anoxic event 2 triggered by a massive magmatic episode. *Nature* **454**, 323–327 (2008).

10 Palmer, M. R. & Edmond, J. M. Controls over the strontium isotope composition of river water. *Geochim. Cosmochim. Acta* **56**, 2099-2111 (1992).

11 Galy, A., France-Lanord, C. & Derry, L. A. The strontium isotopic budget of Himalayan Rivers in Nepal and Bangladesh. *Geochim. Cosmochim. Acta* **63**, 1905–1925 (1999).

12 Huh, Y. in *Monsoon Evolution and Tectonics – Climate Linkage in Asia* Vol. 342 (eds P. D. Clift, A. Tada, & H. Zheng) 129–151 (2010).

13 Marriott, C. S., Henderson, G. M., Belshaw, N. S. & Tudhope, A. W. Temperature dependence of δ^7Li, $\delta^{44}Ca$ and Li/Ca during growth of calcium carbonate. *Earth Planet. Sci. Lett.* **222**, 615–624 (2004).

14 Pogge von Strandmann, P. A. E., Burton, K. W., James, R. H., van Calsteren, P. & Gislason, S. R. Assessing the role of climate on uranium and lithium isotope behaviour in rivers draining a basaltic terrain. *Chem. Geol.* **270**, 227–239 (2010).

15 Vigier, N. *et al.* Quantifying Li isotope fractionation during smectite formation and implications for the Li cycle. *Geochim. Cosmochim. Acta* **72**, 780–792 (2008).

16 Burton, K. W. & Vigier, N. in *Handbook of Environmental Isotope Geochemistry* (ed M. Baskaran) 41–59 (Springer, 2011).

17 Tomascak, P. B. in *Geochemistry of Non-Traditional Stable Isotopes* Vol. 55 *Reviews in Mineralogy & Geochemistry* (eds C. M. Johnson, B. L. Beard, & F. Albarède) 153–195 (2004).

18 Kisakürek, B., James, R. H. & Harris, N. B. W. Li and δ^7Li in Himalayan rivers: Proxies for silicate weathering? *Earth Planet. Sci. Lett.* **237**, 387–401 (2005).

19 Millot, R., Vigier, N. & Gaillardet, J. Behaviour of lithium and its isotopes during weathering in the Mackenzie Basin, Canada. *Geochim. Cosmochim. Acta* **74**, 3897–3912 (2010).

20 Elliott, T., Thomas, A., Jeffcoate, A. & Niu, Y. L. Lithium isotope evidence for subduction-enriched mantle in the source of mid-ocean-ridge basalts. *Nature* **443**, 565–568 (2006).

21 Teng, F. Z. *et al.* Lithium isotopic composition and concentration of the upper continental crust. *Geochim. Cosmochim. Acta* **68**, 4167–4178 (2004).
22 Lemarchand, E., Chabaux, F., Vigier, N., Millot, R. & Pierret, M. C. Lithium isotope systematics in a forested granitic catchment (Strengbach, Vosges Mountains, France). *Geochim. Cosmochim. Acta* **74**, 4612-4628 (2010).
23 Huh, Y., Chan, L. H. & Edmond, J. M. Lithium isotopes as a probe of weathering processes: Orinoco River. *Earth Planet. Sci. Lett.* **194**, 189–199 (2001).
24 Pogge von Strandmann, P. A. E. *et al.* Riverine behaviour of uranium and lithium isotopes in an actively glaciated basaltic terrain. *Earth Planet. Sci. Lett.* **251**, 134–147 (2006).
25 West, A. J., Galy, A. & Bickle, M. Tectonic and climatic controls on silicate weathering. *Earth Planet. Sci. Lett.* **235**, 211–228 (2005).
26 Hathorne, E. C. & James, R. H. Temporal record of lithium in seawater: a tracer for silicate weathering? *Earth Planet. Sci. Lett.* **246**, 393–406 (2006).
27 Misra, S. & Froelich, P. N. Lithium Isotope History of Cenozoic Seawater: Changes in Silicate Weathering and Reverse Weathering. *Science* **335**, 818–823 (2012).
28 Pogge von Strandmann, P. A. E. *et al.* Lithium, magnesium and silicon isotope behaviour accompanying weathering in a basaltic soil and pore water profile in Iceland. *Earth Planet. Sci. Lett.* **339–340**, 11–23 (2012).
29 Jarvis, I., Gale, A. S., Jenkyns, H. C. & Pearce, M. A. Secular variation in Late Cretaceous carbon isotopes: a new $\delta^{13}C$ carbonate reference curve for the Cenomanian– Campanian (99.6–70.6 Ma). *Geological Magazine* **143**, 561–608 (2006).
30 Jenkyns, H. C., Matthews, A., Tsikos, H. & Erel, Y. Nitrate reduction, sulfate reduction, and sedimentary iron isotope evolution during the Cenomanian-Turonian oceanic anoxic event. *Paleoceanography* **22**, PA3208, doi:10.1029/2006PA001355 (2007).
31 Tsikos, H. *et al.* Carbon-isotope stratigraphy recorded by the Cenomanian-Turonian Oceanic Anoxic Event: correlation and implications based on three key localities. *Journal of the Geological Society* **161**, 711–719 (2004).
32 Sageman, B. B., Meyers, S. R. & Arthur, M. A. Orbital time scale and new C-isotope record for Cenomanian-Turonian boundary stratotype. *Geology* **34**, 125–128, doi:10.1130/g22074.1 (2006).
33 Voigt, S., Gale, A. S. & Flögel, S. Midlatitude shelf seas in the Cenomanian-Turonian greenhouse world: Temperature evolution and North Atlantic circulation. *Paleoceanography* **19, PA4020**, doi:10.1029/2004PA001015 (2004).
34 Zhang, L., Chan, L.-H. & Gieskes, J. M. Lithium isotope geochemistry of pore waters from ocean drilling program Sites 918 and 919, Irminger Basin. *Geochim. Cosmochim. Acta* **62**, 2437-2450 (1998).
35 James, R. H. & Palmer, M. R. Marine geochemical cycles of the alkali elements and boron: The role of sediments. *Geochim. Cosmochim. Acta* **64**, 3111–3122 (2000).

36 Scholz, F. *et al.* Lithium isotope geochemistry of marine pore waters – Insights from cold seep fluids. *Geochim. Cosmochim. Acta* **74**, 3459–3475 (2010).
37 McArthur, J. M. *et al.* in *High resolution Stratigraphy* Vol. 70 *Geological Society of London Special Publication* 195–209 (1993).
38 Marriott, C. S., Henderson, G. M., Crompton, R., Staubwasser, M. & Shaw, S. Effect of mineralogy, salinity, and temperature on Li/Ca and Li isotope composition of calcium carbonate. *Chem. Geol.* **212**, 5–15 (2004).
39 Peucker-Ehrenbrink, B. & Ravizza, G. The marine osmium isotope record. *Terra Nova* **12**, 205–219 (2000).
40 Huber, B. T., Norris, R. D. & MacLeod, K. G. Deep-sea paleotemperature record of extreme warmth during the Cretaceous. *Geology* **30**, 123-126, doi:10.1130/0091-7613(2002)030<0123:dsproe>2.0.co;2 (2002).
41 Sahagian, D. Epeorogenic motions of Africa as inferred from Cretaceous shoreline deposits. *Tectonics* **7**, 125–138, doi:10.1029/TC007i001p00125 (1988).
42 Vigier, N., Gislason, S. R., Burton, K. W., Millot, R. & Mokadem, F. The relationship between riverine lithium isotope composition and silicate weathering rates in Iceland. *Earth Planet. Sci. Lett.* **287**, 434–441 (2009).
43 Kuroda, J. *et al.* Contemporaneous massive subaerial volcanism and late Cretaceous Oceanic Anoxic Event 2. *Earth Planet. Sci. Lett.* **256**, 211–223 (2007).
44 Wimpenny, J. *et al.* The behaviour of Li and Mg isotopes during primary phase dissolution and secondary mineral formation in basalt. *Geochim. Cosmochim. Acta* **74**, 5259-5279 (2010).
45 Monteiro, F. M., Pancost, R. D., Ridgwell, A. & Donnadieu, Y. Nutrients as the dominant control on the spread of anoxia and euxinia across the Cenomanian-Turonian oceanic anoxic event (OAE2): Model-data comparison. *Paleoceanography* **27, PA4209**, doi:10.1029/2012PA002351 (2012).
46 Gíslason, S. R., Arnorsson, S. & Armannsson, H. Chemical weathering of basalt in southwest Iceland: Effects of runoff, age of rocks and vegetative/glacial cover. *Am. J. Sci.* **296**, 837–907 (1996).
47 Gíslason, S. R., Oelkers, E. & Snorrason, A. Role of river-suspended material in the global carbon cycle. *Geology* **34**, 49–52 (2006).
48 Courtillot, V. E. & Renne, P. R. On the ages of flood basalt events. *C. R. Geosci.* **335**, 113–140 (2003).
49 Dessert, C., Dupre, B., Gaillardet, J., Francois, L. M. & Allegre, C. J. Basalt weathering laws and the impact of basalt weathering on the global carbon cycle. *Chem. Geol.* **202**, 257–273 (2003).
50 Gaillardet, J., Dupré, B. & Allègre, C. J. Geochemistry of large river suspended sediments: silicate weathering or recycling tracer? *Geochim. Cosmochim. Acta* **63**, 4037–4051 (1999).

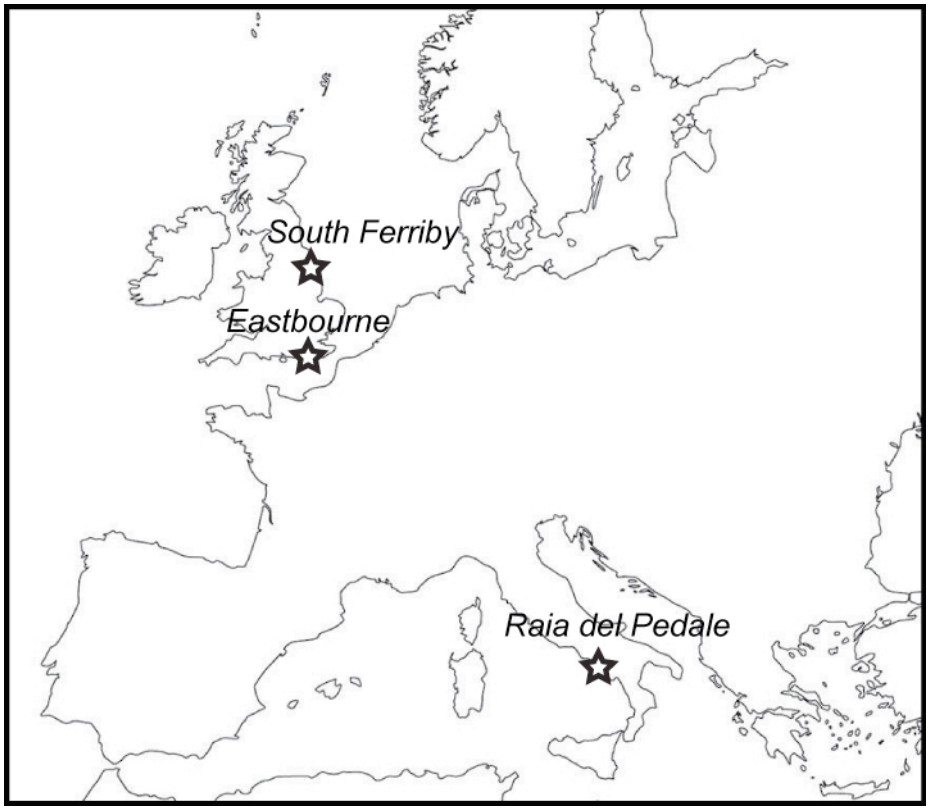

Figure 1. Sample location map. The Trunch borehole is also shown, where Sr isotope ratios correlated to samples in Eastbourne were obtained (Fig. 2).

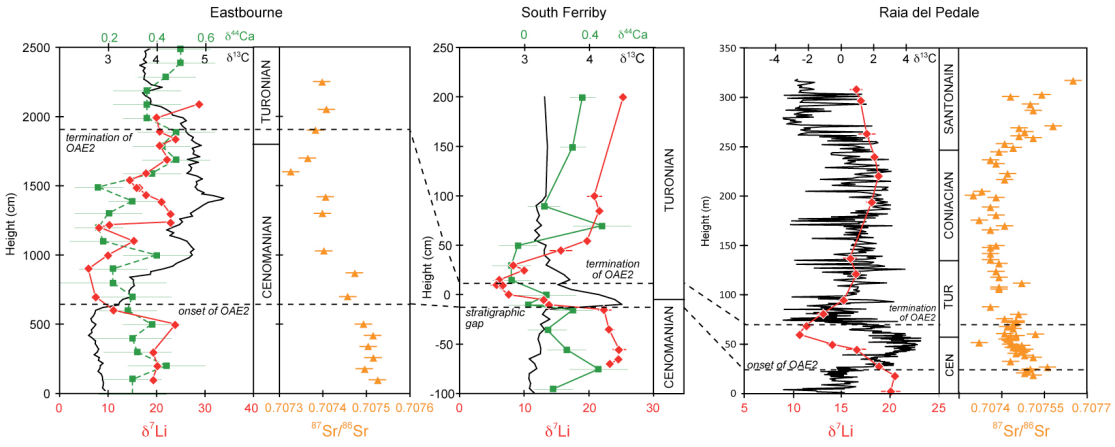

Figure 2. Li isotope ratios of the marine carbonate sections measured in this study: Eastbourne (a), South Ferriby (b) and Raia del Pedale (c). Also plotted are C and Ca isotope ratios[8,31] from the Chalk sections in the UK. Sr and C isotopes from Raia del Pedale are used for correlative purposes.

Sr isotopes for Eastbourne are from the Trunch Borehole, Norfolk, UK[37], covering the same interval using C isotope stratigraphy to correlate with Eastbourne. Sr isotope data from the Trunch Borehole are also used to elucidate stage boundaries in Raia del Pedale, which largely lacks biostratigraphically useful fossils. The C isotope data from Raia del Pedale are readily correlated with Eastbourne and well define the OAE. The South Ferriby section contains a stratigraphic gap indicated by the incomplete carbon isotope profile[30].

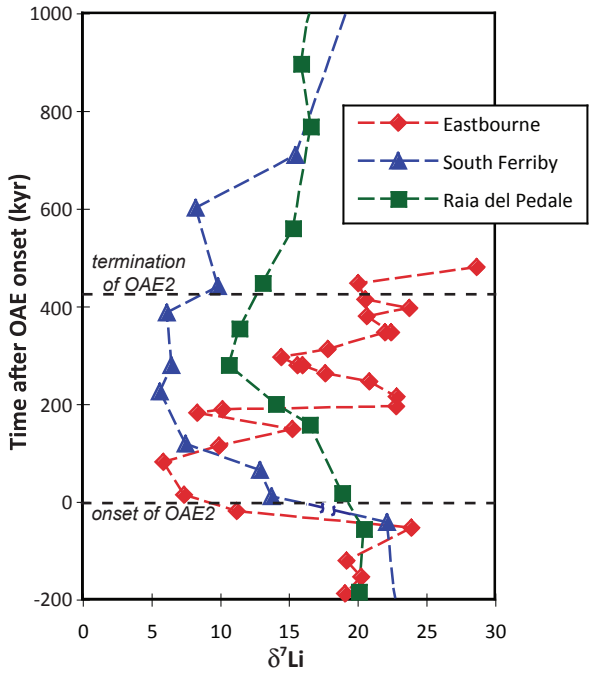

Figure 3. Expanded view of the Li isotope excursions from all analysed sections, plotted against time after onset of the C–T OAE. The timing is based on the assumption that the duration of the carbon isotope excursion is ~440 kyr[6], and that the sedimentation rate is constant. Note that the South

Ferriby section has an unconformity immediately below the start of the carbon isotope excursion, and hence its stratigraphic alignment may be offset.

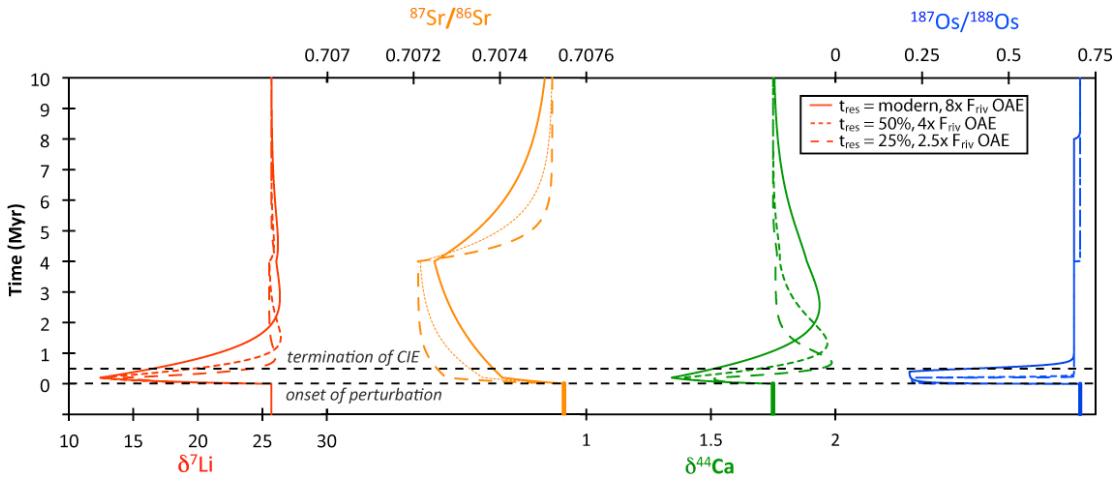

Figure 4. Final best-fit dynamic model of Li, Sr, Ca and Os isotopes. See supplementary information for model details, and intermediate results. The model shown was generated by assuming a 20% hydrothermal increase for 4Myr (constrained by $^{87}Sr/^{86}Sr$, which is the most sensitive system to hydrothermal input), and a transitory enhanced weathering pulse for 200kyr for Li, and other river fluxes increased in proportion to match weathering of fresh basalt. The model shows the results from different ocean residence times, where lower values allow faster recovery and lower enhanced riverine fluxes during the OAE, rendering them more likely representations of the C–T OAE. Note that the models reflect seawater isotope ratios, so calcite fractionation factors are already applied for Li (5‰) and Ca (1.3‰) isotopes, in contrast to Fig. 2.